

## Study of Flow Characteristics in a Closed-Loop Low-Speed Wind Tunnel

Ahmad, A., Sutardi\*, Romi D K N, Fahmi F H, Abel B A, and Anastasia EP

Department of Mechanical Engineering, Institut Teknologi Sepuluh Nopember, Surabaya 60111, Indonesia

Received: 1 June 2017, Revised: 12 July 2017, Accepted: 16 August 2017

### Abstract

Wind tunnel is an element or experimental device that plays an important role in the development of aerodynamics. In general, there are two types of wind tunnels: open-loop wind tunnels and closed-loop wind tunnels. Furthermore, based on the flow velocity in the wind tunnel, the wind tunnel can also be categorized into several types: low-speed wind tunnel and high-speed wind tunnel, including sub-sonic and supersonic wind tunnels. In this study it is used a low-speed closed-loop wind tunnel type. The maximum attainable velocity of airflow in the wind tunnel is about 46 m/s with turbulence intensity (TI) as low as 0.41 percent. The flow parameters that being evaluated in this study include the velocity profiles and intensity of turbulence (TI) in some parts or sections of the wind tunnel. Pressure measurements in the wind tunnel are performed using a Pitot tube connected to a calibrated pressure transducer. The measured values of pressures are then converted into the fluid velocities and turbulence intensities. The results show that the flow quality in the main test section of the wind tunnel is good enough. The intensity of the flow turbulence on the inlet side of the test section is about 0.41 percent at the centerline velocity of approximately 40 m/s. In some parts of the wind tunnel, turbulence intensity is still relatively high, as in the small elbow outlet where TI is higher than 18 percent.

**Keywords:** Low speed wind tunnel, Turbulence, Wind tunnel.

### 1. Introduction

In terms of construction, the wind tunnel is categorized into two types: (i) open loop wind tunnel and (ii) closed loop wind tunnel. Open-loop wind tunnels are widely used, both within research institutions, industries, and in educational institutions. This open-type wind tunnel is simpler and easier to build. The closed-type wind tunnel is relatively more complicated in its design, so that the users of closed-type wind tunnels are not as many as the users of the open type wind tunnels. In closed-type wind tunnels, it can also be guaranteed better fluid flow quality than flow quality in the open-type wind tunnels. The quality of this flow includes the intensity of turbulence and vibration of the wind tunnel construction.

In terms of power or energy consumption, the closed-type wind tunnels are more efficient than the open-type wind tunnels for the same capacity and test section area. From some previous studies, it was shown that for a particular fan or blower type, the maximum capacity can be obtained when a closed-type wind tunnel is used. This is because the pressure loss in the open-type one is greater than in the closed-type. Messina [1] found that a particular fan in a closed-type wind tunnel is capable of generating a capacity of about 11 percent higher compared to an open-type wind tunnel.

The main component of wind tunnel that generates

the greatest loss is the diffuser located downstream of the test section. The contribution of pressure losses to the diffuser is more than 30 percent of the total pressure loss. The component that contributes to the second largest pressure loss is the elbows in the closed-type wind tunnel channel, which contributes up to approximately 16 percent of total pressure losses. Therefore, a study of pressure loss in a wind tunnel design needs to be thoroughly performed in order to obtain an efficient design of a wind tunnel but capable of producing maximum flow quality. There have been many studies of the wind tunnel design, both open-type and closed-type, as shown in Lingdren and Johansson [2], Barlow et al. [3], and Mehta and Bradshaw [4].

In this study we examine the characteristics of the airflow within a closed-type, or also frequently referred to as closed-loop, wind tunnel, where analysis are focused on the velocity profiles and intensity of turbulence in some parts of the wind tunnel.

### 2. Methods

The experiment was conducted at the Fluid Mechanics Laboratory of Mechanical Engineering Department, ITS Surabaya. The main equipment of this experiment is a closed-loop low-speed wind tunnel, where the air flow is driven by an axial fan with input power of 4 kW with a motor speed of 2800 rpm. The resulting flow capacity is up to

\*Email: [sutardi@me.its.ac.id](mailto:sutardi@me.its.ac.id)  
Phone: +6281

15000 m<sup>3</sup>/hr. With this large flow capacity, the maximum airflow velocity that can be reached in the test section is approximately 46 m/sec. The turbulence intensity of the centerline test section is 0.46 percent at 32 m/sec. Figure 1 shows a schematic diagram of the wind tunnel used in this study.

The geometry of the honey comb, screen mesh, and nozzle is simply shown in Figure 2. The nozzle is designed to produce a smoother flow when entering the test section. Smooth outflow from the nozzle can be aided by the addition of honey comb and screen mesh (screen mesh). Size and material nozzle is as follows:

- Nozzle wall material : Fiber, 5 mm thick
- Inlet height  $H_{i,N}$  : 770.5 mm
- width  $W_{i,N}$  : 770.5 mm
- Outlet height  $H_{N,exit}$  : 300 mm
- Outlet width  $W_{N,exit}$  : 300 mm
- Nozzle length  $L_N$  : 1000 mm
- Nozzle area ratio  $AR_{Nozzle}$  : 6.6

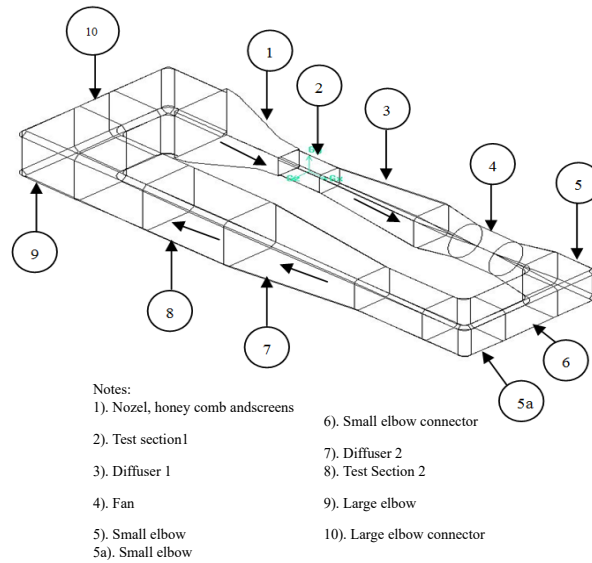


Figure 1. Schematic diagram of a closed-loop low speed wind tunnel

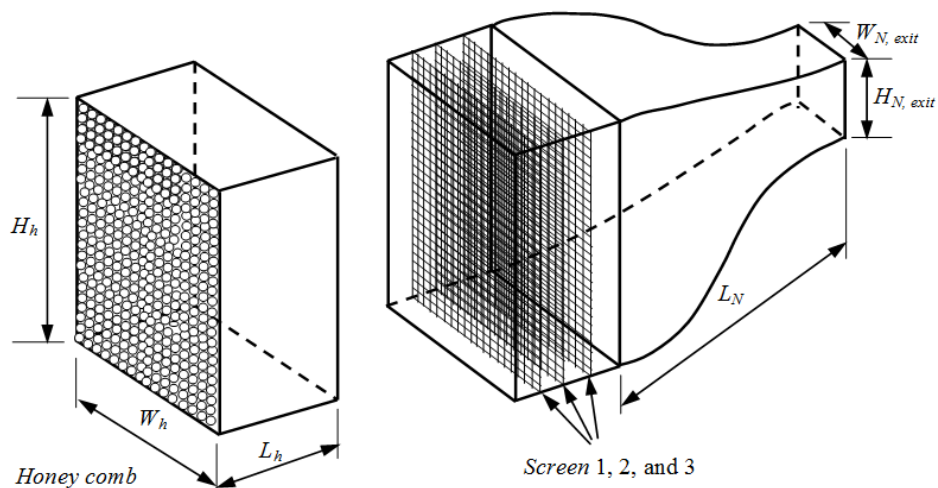


Figure 2. Honey comb, screen mesh, and nozzle construction.

Velocity measurements are performed using a Pitot tube connected with a pressure transducer that has been calibrated. Pressure transducer calibration is conducted using an inclined manometer (inclined angle,  $\varphi = 15^\circ$ ) filled with red oil ( $SG = 0.827$ ). Pressure transducer has a measurement range of up to 5 inches of water column. The differential pressure read on the pressure transducer is then converted to velocity and then processed to obtain local velocity values and local turbulence intensity. The sampling rate is 25 measurement data per second and as many as 500 data were used for turbulence measurements.

### 3. Results and Discussion

#### 3.1. Velocity Profiles

The flow phenomenon in the symmetric nozzle at  $ReD_h = 4.68 \times 10^5$  can be seen in Figure 3. It is shown that the velocity distribution of the experimental results in the symmetric nozzle is expressed in non-dimensional forms of velocity ( $u/U_{max}$ ) and distance from the wall ( $y/w_1$ ) for several streamwise distances ( $x/L_1$ ). In this case,  $L$  is the nozzle total length,  $w_1$  is the half width of the nozzle at a particular cross-section, and  $x$  is measured from the nozzle inlet. The total length of the nozzle ( $L$ ) is 630 mm. The value ( $u/U_{max}$ ) is ratio between local velocity magnitude in the prescribed cross-section to the maximum  $u$  at the same cross-section.

From the velocity profiles, it can be seen that the profiles show a high turbulent level of the flow stream, indicated by almost uniform velocity profiles at all cross-sections considered in this study. Although the profiles show high turbulent level, the intensity of turbulence at the nozzle exit is considered to be low, as will be described

in the next discussion. As shown in the figure, the development of the boundary layer thickness is very small as fluid flows from the nozzle inlet to the nozzle outlet (entering the test section).

Figures 4a to c show velocity profiles distribution in the wind tunnel main test section and three different stream-wise locations  $x = 70$  mm, 140 mm, and 250 mm, where  $x$  is measured from the test section inlet. There are four centerline velocities used to examine the velocity profiles, i.e.: 10 m/sec, 20 m/sec, 30 m/sec, and 40 m/sec. There freestream velocities correspond with the flow Reynolds numbers, based on the test section hydraulic diameter,  $D_h$ , of  $1.94 \times 10^5$ ,  $3.87 \times 10^5$ ,  $5.81 \times 10^5$ , and  $7.74 \times 10^5$ , respectively. Hence, the flow can be considered as the high Reynolds number flows. Dash lines show approximation profiles for power-law equation, at least up to the edge of the boundary layer thickness ( $\sim 2$  cm). In this case, the power-law profile can be expressed as:

$$u/U_0 = (y/\delta)^{1/6} \quad (1)$$

where  $\delta$  is the boundary layer thickness. Among these three profiles, the profiles at  $x = 140$  mm and 250 mm are having the best agreement with the power-law equation as shown in equation 1. However, the profile at the first  $x$ -location ( $x = 70$  mm), the profile seems to more appropriate if it is approximated with power slightly higher than that of shown in equation 1. The power of the equation for the profile is probably seems to be one-seventh ( $1/7$ ). This is indicated that the 1<sup>st</sup> profile is flatter in the near-wall region compared to the 2<sup>nd</sup> and the 3<sup>rd</sup> profiles.

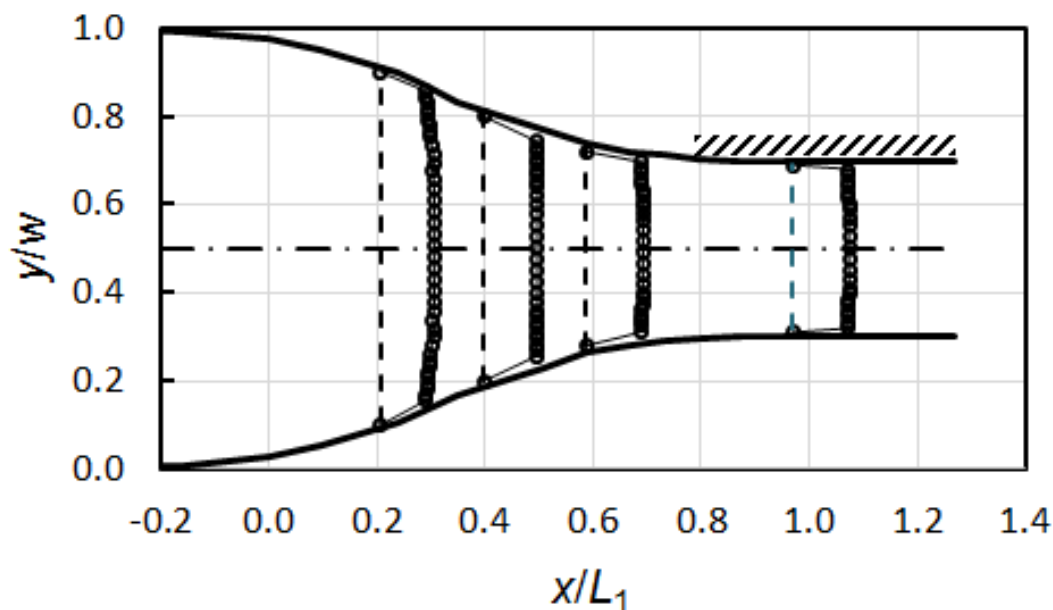
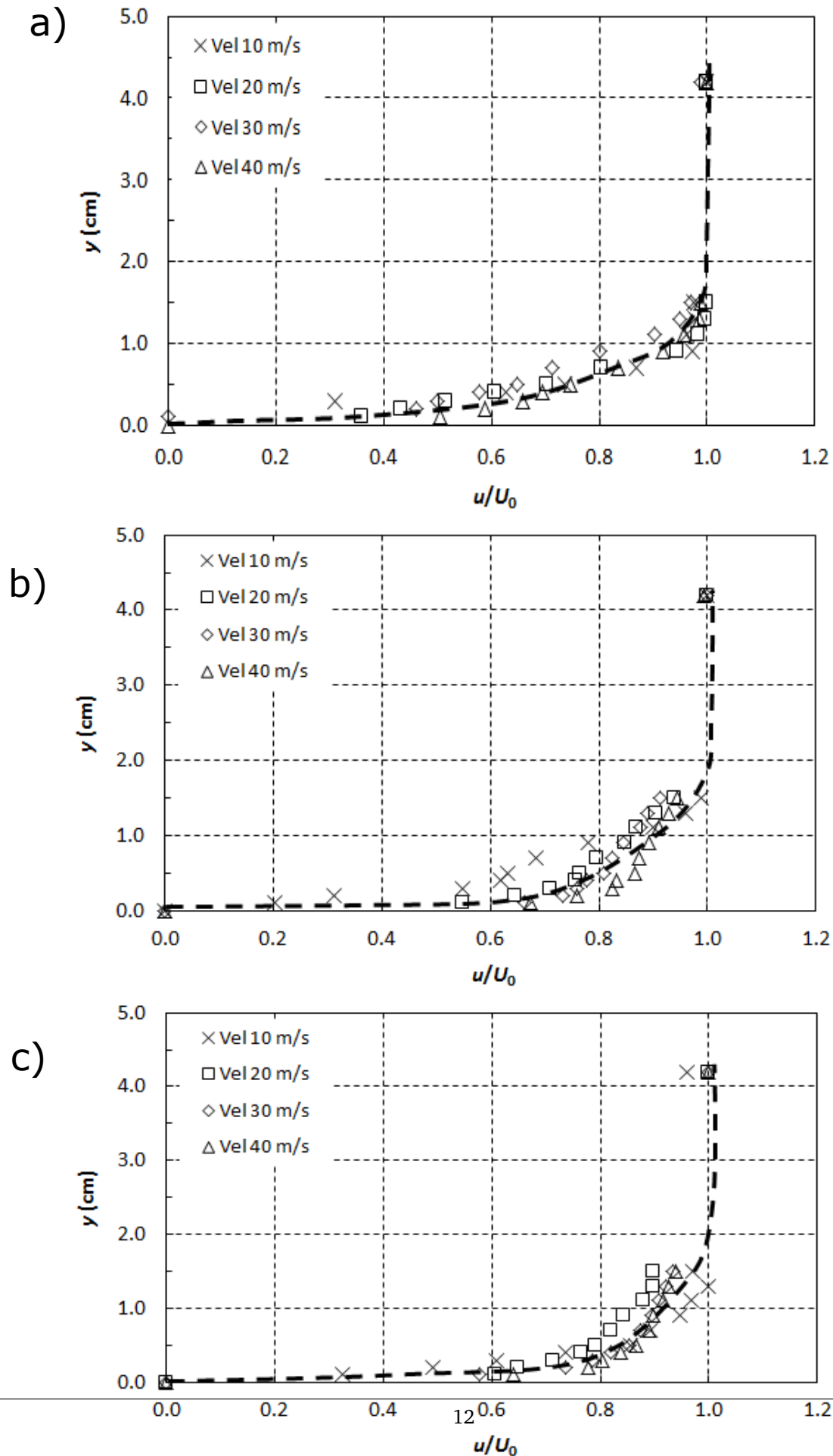


Figure 3. Velocity profiles at four cross-sections in the nozzle section of the closed-loop wind tunnel.



**Figure 4.** Velocity profiles distribution in the wind tunnel main test section and three different streamwise locations: (a). 1<sup>st</sup> point ( $x = 70$  mm), (b). 2<sup>nd</sup> point ( $x = 140$  mm), and (c). 3<sup>rd</sup> point ( $x = 250$  mm).

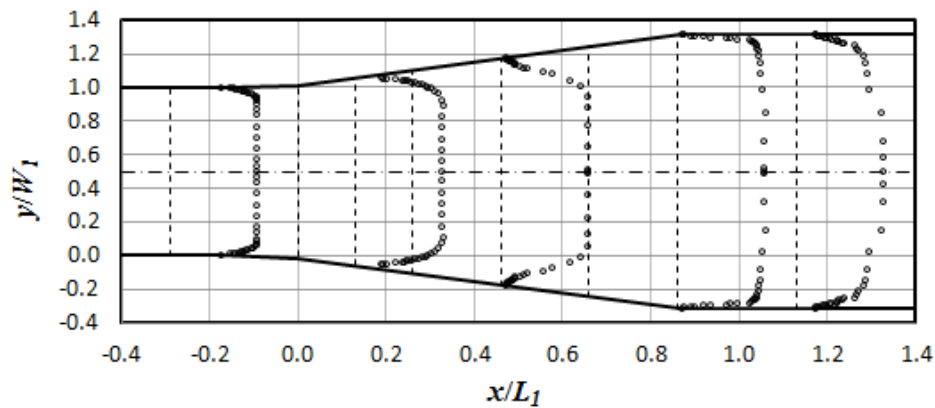


Figure 5. Velocity profiles at  $Re_{Dh} = 3,86 \times 10^5$  in the small diffuser.

Figure 5 shows the distribution of the velocity profile in the small diffuser (part 3 in Figure 1), ( $U/U_{max}$ ) at  $Re_{Dh} = 3.86 \times 10^5$ . In this case,  $U_{max}$  has the same meaning as  $U_0$ , that is the maximum velocity at the channel centerline. From the figure it is seen that no indications of flow separation on the diffuser wall. This shows that the diffuser has a good performance in terms of flow control, which responsible to the process of flow kinetic energy conversion into the flow pressure energy of fluid flow through the diffuser. Therefore, the performance of this diffuser is good enough to be used in a wind tunnel.

The minor losses coefficient ( $K_L$ ), that is defined as  $K_L = 2\Delta P / (\rho(V_{in})^2)$  of this diffuser is approximately 0.21~0.26 within the  $Re_{Dh}$  used in the study. In this case,  $V_{in}$  is the fluid average velocity at the diffuser inlet. This value is slightly different from the  $U_{max}$  or  $U_0$ . Overall, the velocity profile distribution remains symmetry within the flow domain. Based on the diffuser geometry, with the opening angle  $(2\theta) = 8^\circ$ , as well as the ratio of the dif-

fuser length to the inlet width  $(L/b)_{in} = 5.0$ , this diffuser is in the "no-stall" performance map region (see Figure 1). It can be understood that the pressure loss in the diffuser is mostly contributed by viscosity rather than by secondary flow or flow separation.

Figure 6 shows the velocity profiles ( $U/U_{max}$ ) on the inlet side of the small elbow (section 5a in Figure 1), at two  $Re_{Dh}$ . Parameter  $(r - r_1)/b = 0$  is the location at the inner radius of the elbow, while parameter  $(r - r_1)/b = 1$  is the location at the outer radius of the elbow. It is shown that there is an acceleration of flow at the outer radius of the elbow. This is due to the influence of the other small elbow located at the upstream side of the elbow that is being evaluated (Section 5 of Figure 1). Since the distance of elbow 5 and elbow 5a is quite close, the effect of elbow 5 on elbow 5a cannot be avoided. In subsequent studies, this un-uniformity of the velocity distribution is minimized by the addition of the guide vanes inside the elbow.

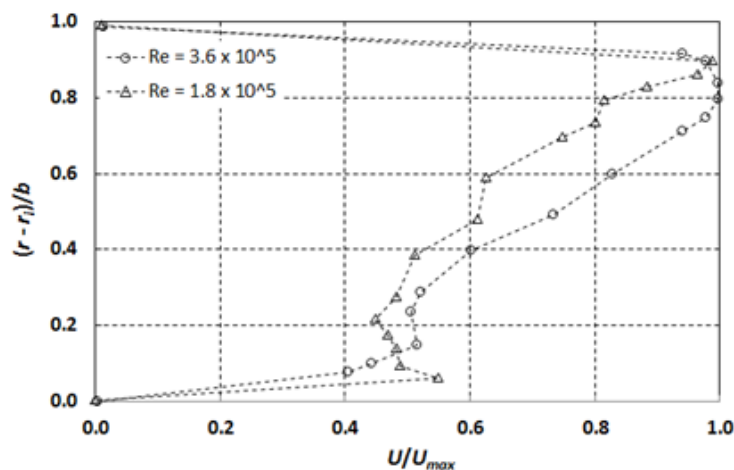


Figure 6. Velocity profiles at the inlet section of the small elbow at two values of  $Re_{Dh}$ .

### 3.2. Turbulence Intensity

The velocity fluctuations in the centerline of the wind tunnel main test section (no. 2 in Figure 1) for the three axial locations are shown in Figure 7a to 7c. These three locations are at the nozzle exit, at the middle of the test section, and at the outlet of the test section or the inlet of the small diffuser, respectively (see also Figure 1). The turbulence intensity in this case is calculated using the following equation:

$$TI = \frac{U_{rms}}{\bar{U}} \times 100 \quad (2)$$

$$\overline{U_{rms}} = \sqrt{(U'(t) - \bar{U})^2} \quad (3)$$

where:

$U_{rms}$  : root-mean square of the fluctuating velocity (m/s),

$\bar{U}$  : mean velocity, m/s, and

$U'$  : instantaneous velocity (t), m/s.

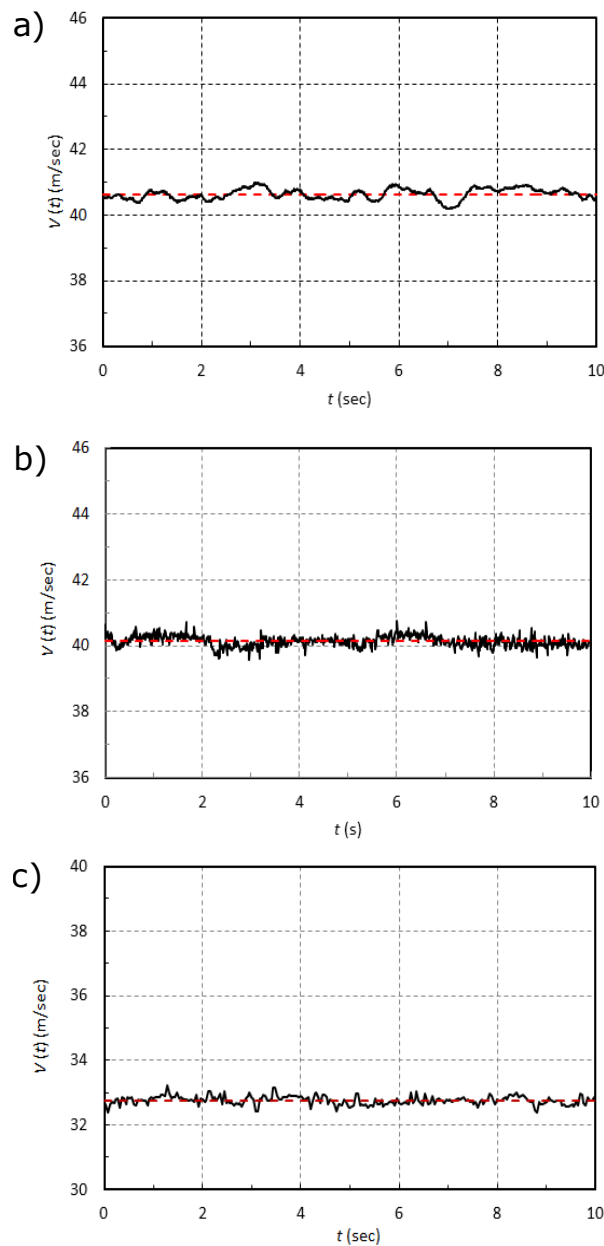
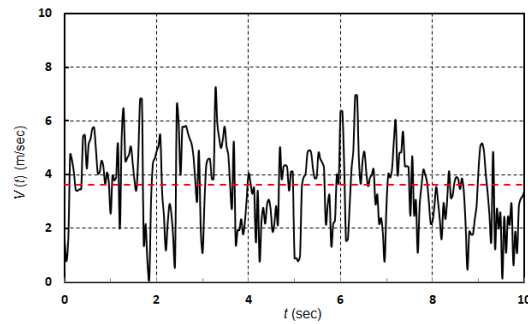


Figure 7. Velocity fluctuations in the centerline of the wind tunnel main test section.



**Figure 8.** Velocity fluctuations at the large elbow outlet,  $U = 3.61$  m/sec, with  $TI = 39.3\%$ .

Figure 7a shows the velocity signal at the inlet of the test section, with average velocity ( $U$ ) of approximately of 40.6 m/sec., with its turbulence intensity of approximately 0.410 m/sec. At the second section (Figure 7b), the data were taken at slightly different average velocity, that is 40.2 m/s with its turbulence intensity of 0.407 m/sec. The distance between section (1) (the velocity signal as shown in Figure 7a) and section (2) (the velocity signal as shown in Figure 7b), is approximately 70 mm, with constant value of cross section. Based on these data, we can see that the quality of the average velocity and the turbulence intensity in the test section are considered to be very good.

Next, Figure 7(c) shows the velocity fluctuation in the end of the test section. At this section, the average velocity of approximately 32.7 m/s and the turbulence intensity is about 0.49%. At this section, it was intentionally that the data were taken at different average velocity to show the consistence of the value of the turbulence intensity in the test section. It was shown that, although there is slightly increase in the turbulence intensity from 0.410 m/sec to 0.490 m/sec, at the inlet and at the outlet of the test section, respectively, the increase is to be small. The slight increment in this turbulence intensity is due to the lower value of the average velocity at the end section (32.7 m/s) comparing to the inlet section (40.6 m/s). Furthermore, all values of the turbulence intensity in the test section ( $< 0.5\%$ ) is considered to be very small and the

airflow in the test section is very good in quality.

This turbulence intensity is considered quite low for the size of wind tunnel in general. This indicates that the process of flow re-laminarization occurring in the wind tunnel nozzle (component no. 1 in Figure 1) is quite successful. Based on information obtained from Cebeci and Smith [5], wind tunnel with this turbulence intensity can be categorized as good enough for wind tunnel in general, even if the intensity value is not as low as 0.2%.

Furthermore, Figure 8 shows the velocity fluctuation at the large elbow inlet (component no. 9 in Figure 1), with an average velocity ( $U$ ) of approximately 3.61 m/s, with its turbulence intensity of about 39.3%. This turbulence intensity value is very high at this location, which is the result of the effect of the presence some components at the upstream side of this location. These components include large diffuser (component no. 7), two small elbows (components no. 5 and 5a), and the axial fan (component no 4). The increase of turbulence intensity is also as the results of the lower average velocity at this location.

The measurement of velocity fluctuations is also performed in several other axial locations in the wind tunnel, as at the outlet side of the small diffuser, at the outlet side of the small elbow, and at the outlet side of the large elbow. However, the plots of the velocity fluctuations are not shown in this paper, but the values of turbulence intensities ( $TI$ ) are presented in the table as shown in Table 1.

2

**Table 1.** Turbulence intensities at several centerline locations in the wind tunnel

Location	Turbulence Intensity (TI, %)
Test section	0.41 ( $Re_{Dh} = 7.9 \cdot 10^5$ )
Small diffuser inlet	0.49 ( $Re_{Dh} = 5.8 \cdot 10^5$ )
Small elbow outlet	18.65 ( $Re_{Dh} = 1.8 \cdot 10^5$ )
	5.31 ( $Re_{Dh} = 3.6 \cdot 10^5$ )
Large diffuser outlet	13.97 ( $Re_{Dh} = 3.1 \cdot 10^5$ )
Large elbow outlet	39.30 ( $Re_{Dh} = 1.8 \cdot 10^5$ )

#### 4. Conclusions

From the study of fluid flow in a closed-loop low-speed wind tunnel, we can obtain some conclusions as follows:

1. The intensity of turbulence (TI) inside the main test section (section no. 2 in Figure 1) is quite low, that is approximately 0.41% at  $Re_{Dh} = 7.9 \times 10^5$ .
2. The performance of the small diffuser is good enough with no symptoms of flow separation therein, at least at the Reynolds numbers used in the experiment.
3. The elbow plays a significant role in altering the uniformity of the flow in the particular wind tunnel cross section.
4. The use of the nozzle equipped with honey comb and mesh screens proves to be effective to reduce the flow turbulence.

#### References

- [1] M. Messina, "Experimental validation of pressure loss in anemometer testing equipment," *Renewable and Sustainable Energy Reviews*, vol. 16, no. 5, pp. 2980–2987, 2012.
- [2] B. Lindgren and A. V. Johansson, "Design and evaluation of a low-speed wind-tunnel with expanding corners," *Department of Mechanics, KTH, Report No. TRITA-MEK*, vol. 14, 2002.
- [3] J. B. Barlow, W. Rae, and A. Pope, "Low-speed wind tunnel testing, 1999," *Jhon Wiley & Sons, Canada*.
- [4] R. D. Mehta and P. Bradshaw, "Design rules for small low speed wind tunnels," *The Aeronautical Journal*, vol. 83, no. 827, pp. 443–453, 1979.
- [5] T. Cebeci, A. Smith, and P. Libby, "Analysis of turbulent boundary layers," *Journal of Applied Mechanics*, vol. 43, p. 189, 1976.